Comparative Studies of Using Nano Zerovalent Iron, Activated Carbon, and Green Synthesized Nano Zerovalent Iron for Textile Wastewater Color Removal Using Artificial Intelligence, Regression Analysis, Adsorption Isotherm, and Kinetic Studies

Comparative Studies of Using Nano Zerovalent Iron, Activated Carbon, and Green Synthesized Nano Zerovalent Iron for Textile Wastewater Color Removal Using Artificial Intelligence, Regression Analysis, Adsorption Isotherm, and Kinetic Studies

Ahmed Karam[1] (iD), Khaled Zaher[2] and Ahmed S Mahmoud[3] (iD)

[1]Department of Civil & Infrastructure Engineering & Management, Nile University, Giza, Egypt.
[2]Sanitary and Environmental Engineering, Department of Civil Engineering, Faculty of Engineering, Cairo University, Giza, Egypt. [3]Sanitary and Environmental Institute (SEI), Housing and Building National Research Center (HBRC), Giza, Egypt.

ABSTRACT: Daily, a big extent of colored, partially treated textile effluents drained into the sanitation systems causing serious environmental concerns. Therefore, the decolorization treatment process of wastewater is crucial to improve effluent quality. In the present study, 3 different sorbent materials, nano zerovalent iron (nZVI), activated carbon (AC), and green-synthesized nano zerovalent iron (GT-nZVI), have been prepared for raw textile wastewater decolourization. The prepared nanomaterials were characterized via X-ray diffraction (XRD) spectroscopy, scanning electron microscopy (SEM), energy dispersive X-ray (EDX) analysis, and UV-Vis absorption spectroscopy. In addition, the effect of different operating parameters such as pH, contact time, and stirring rate on the color removal efficiency was extensively studied to identify the optimum removal conditions. The reaction temperature, adsorbent dose, and initial color concentration were fixed during the experiments at room temperature, 0.7 g/L, and 350 and 50 mg/L Pt/Co color unit, respectively. Moreover, adsorption and reaction kinetics were analyzed using different isotherms and models. For simulating the adsorption process, artificial neural network (ANN) data were compatible with the result of regression analysis derived from response surface methodology (RSM) optimization. Our results showed the higher ability of nZVI, AC, and GT-nZVI in textile wastewater color removal. At pH 5, contact time 50 minutes, and stirring rate 150 rpm, nZVI showed good color removal efficiency of about 71% and 99% for initial color concentrations of 350 and 50 mg/L Pt/Co color unit, respectively. While slightly higher color removal ability of about 72% and 100% was achieved by using AC at pH 8, contact time 70 minutes, and stirring rate 250 rpm. Finally, the largest ability of color removal about 85% and 100% was recorded for GT-nZVI at pH 7, contact time 40 minutes, and stirring rate 150 rpm. This work shows the enhanced color removal ability of GT-nZVI as a potential textile wastewater decolourization material, opening the way for many industrial and environmental applications.

KEYWORDS: Real textile wastewater, color removal, nZVI, AC, GT-nZVI, artificial neural networks, regression analysis, isotherm and kinetic studies

Introduction and Backgrounds

Water is the secret of life for every living thing. It was accounted that about 97.5% of the whole accessible water on the earth is salty and unfeasible for being used. However, only 1% of the remaining 2.5% freshwaters are considered usable for human consumption.[1,2] The United Nations Environment Program (UNEP) has stated that some African and European countries will be prone to water scarcity troubles by 2025. Moreover, 66% of the world populace could be insecure from the water crisis.[3,4] Water pollution is the foremost cause of water squander as it wastes the chance for water to be reused, particularly these waters that come out of industrial processes.[1,5]

The textile industry is at the forefront of industries consuming and polluting water.[6,7] It devours around 200 m³ of clean water to manufacture only 1 ton of fabric. Furthermore, the drainage of the resulting fabric wastewaters is highly posing a serious environmental impact as it characterized by incredible levels of chemical oxygen demand (COD), biological oxygen demand (BOD), pH along with robust color, and other organic and inorganic constituents.[7,8] Dyes in water are often toxic and has a key impact on causing genotoxicity and carcinogenicity to the aquatic organisms. Moreover, it has devastating effects on humans and public health, and it can amplify the incidence of cancer, hemorrhage, fetus cerebral abnormalities, and dermatitis.[9,10] In this way, dyes elimination from effluents is substantial before discharging to the environment.

Lately, it became a must for industrial factories to comply with the strict environmental laws, which deter poor discharge of industrial effluents.[11] Therefore, numerous factories were considered tertiary treatment to enhance the quality of their effluent, for instance, ozonation,[12] ultrafiltration,[13] nano-filtration,[14] and reverse osmosis.[15] Despite all of these treatment techniques may be effective regarding the removal of dyes, they impact negatively on operational costs as periodic maintenance

is highly obligatory. On the other side, photodegradation is widely considered for the removal of different types of dyes.[16,17] Nevertheless, it possess drawbacks such as fast electron hole recombination, limited visible light response ability, low specific surface area for reaction, and difficult to be implemented in the treatment plants.[18]

Adsorption is one of the highest potential techniques for textile effluent quality enhancement as a result of its simple operation, major elimination of dyes, and contaminants over low cost. Using adsorbent has great adsorption capability and needs little processing.[19-22] Diverse natural materials such as timber sawdust,[23] pine cone,[24] chitosan,[25] and natural clay[8] have a fair adsorption efficiency of dyes from aqueous solutions, but they are incompetent in dealing with such hard complex real textile wastewaters. For raw textile wastewaters, activated carbon (AC) is one of the extensively used adsorbents rather than other materials for COD and color reduction, thanks to its great surface area and marvelous adsorption capability.[26-28]

Recent studies have reported nano zerovalent iron (nZVI) as a highly efficient, less toxic, and cost-effective adsorbent for color removal,[29-32] heavy metals elimination,[33,34] and organic impurities degradation.[35] The reason for this is attributed to the nZVI abundant superior surface area and its great porous structure.[36] On the other side, the application of using nZVI based on green synthesis preparation (GT-nZVI) has been proposed via today's research as a promising eco-friendly economic adsorbent material with massive contaminants removal capability.[37,38] In general, the adsorption process is affected by adsorbent dose, pH, stirring rate, and contact time for real textile wastewater treatment.[19,28] The relationship between experimental factors and the response of interest (removal efficiency) can be evaluated using response surface methodology (RSM).[39] Vargas et al[40] applied RSM to investigate the adsorption performance of 3 dyes such as Acid Yellow 6 (AY-6), Acid Yellow 23 (AY-23), and Acid Red 18 (AR-18) onto AC produced from flamboyant pods (Delonix regia). The RSM well revealed the parameters that effect the ternary adsorption of each dye: pH for AY-23, adsorption time for AR-18, and initial concentration for AY-6 and AR-18.[40] In another study, Ahmed S. Mahmoud et al (2019) studied the reduction of organic matter from municipal wastewater using GT-nZVI. The RSM based on linear regression enter method successfully predicted the correlation between the removal efficiency and different operating conditions.[41]

The impacts of the experimental factors on the adsorption process performance can also be exhibited by artificial neural networks (ANN). Artificial neural networks have indicated an incredible guarantee in driving important connections between off-base data by interfacing input data with one another and with the output data.[41,42] Daneshvar et al[43] have developed an ANN model to predict the decolorization efficiency of the C.I. Basic Yellow 28 using the electrocoagulation process based on experimental data obtained from batch studies. The input parameters such as solution pH and conductivity, current density, initial concentration of dye, time of electrolysis, distance between the electrodes, and retention time were studied to predict the dye removal. They found that simulations based on the developed ANN model can estimate the behavior of the decolorization process under different conditions.[43]

This work attempts to examine the removal of real color from textile wastewater using 3 different sorbent materials nZVI, AC, and GT-nZVI. Batch studies were investigated to determine the effects of pH, adsorbent material dosage, contact time, concentration, and stirring rate for the best adsorption rates of real color. The mechanism of real color adsorption and maximum uptake have been thoroughly discussed by different adsorption isotherm models. Different kinetic models were performed to accurately specify the rate and order of reaction for the 3 studied sorbent materials. Response surface methodology based on linear regression enter method is conducted to reveal the color removal equation rather than optimum conditions. Artificial neural network (ANN) using multilayer perceptron (MLP) statistics algorithms was conducted to detect the relation between experimental factors and real color removal. This study was carried out based on the effluent wastewaters resulting from one of the textile factories in El-Sadat City, Menoufia-Egypt. This factory adopts the chemical treatment method represented in coagulation-flocculation and sedimentation process to treat about 200 m³ of raw textile wastewater daily. The wastewater received by this plant is usually produced from the dyeing and finishing processes of cotton fabrics, which is exceedingly polluted. Unluckily, the treated effluent quality was not as efficient as required by the Egyptian Standards to be discharged to the sewage networks or non-fresh waterways as mentioned in Table 2.

Materials and Methods

Chemicals and reagents

The following chemicals were used in the current study: ferric chloride (FeCl$_3$·6H$_2$O, 98.5% pure; Arabic Lab.), sodium boron hydride (NaBH$_4$, 99% pure; Win Lab.), ethyl alcohol (C$_2$H$_6$O, 95% pure; World Co.), sodium hydroxide (NaOH, 99% pure; Oxford Co.), sulfuric acid (H$_2$SO$_4$, 95%-97%; Honeywell Co.), soft black tea, and activated charcoal (Powder, pH 6-9; Sigma-Aldrich Co.).

Preparations

Preparations of nZVI. About 1.0812 g of ferric chloride (FeCl$_3$·6H2O) was absolutely dissolved in 60 mL 4/1 (v/v) ethanol/deionized water mixture. The reducing agent used was prepared by dissolving exactly 0.7564 g of NaBH$_4$ at 200 mL of deionized water. The reducing NaBH$_4$ solution was poured in a burette and slowly dropped into the FeCl$_3$ solution

with a rate of 1 drop/s. The black precipitate was immediately formed after the initial drops of NaBH$_4$ solution as explained in equation (1). The chemical reduction between NaBH$_4$ and FeCl$_3$ was used to form black nZVI. Following that, the resulting mixture was agitated for further 10 minutes after adding the excess amount of NaBH$_4$ to complete FeCl$_3$ reduction. Then, the normal filtration technique was operated to separate and wash the precipitated iron nanoparticles from the liquid solution using Whatman filter paper (No. 42, 100 circles, diameter 150 mm, and 2.5 μm pore size). Finally, the chemically prepared nZVI was dried at 80°C for 3 hours. For storage, the prepared nZVI was saved against oxidation by adding a layer of acetone[44]:

$$2FeCl_3 + 6NaBH_4 + 18H_2O$$
$$\rightarrow 2Fe^0 + 21H_2 + 6B(OH)_3 + 6NaCl \qquad (1)$$
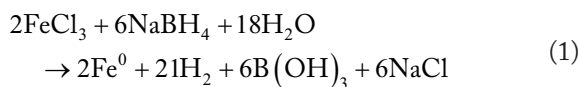
Preparation of GT-nZVI. Synthesis of green synthesized nano zero iron was done by using drop-by-drop method using black tea. About 25 g of soft Kenyan black tea per liter of deionized water was boiled for 2 hours at 200°C, then cooled, and the solution was filtered by filter paper number 1. About 100 mL of extra pure ethanol/acetone solution (1:1) was added to the infiltrated dry tea, mixed for about 15 minutes at normal room temperature, and then filtrated again to extract the tea solution. About 2.3212 g of FeCl$_3$·6H$_2$O was dissolved in deionized water. The extracted prepared tea solution was emptied in a burette and dropped into FeCl$_3$, separated, washed, dried, and stored as detailed in section "Chemicals and Reagents."[45]

Effect of operating parameters

The effect of operating parameters was conducted by using Table 1.

Batch adsorption studies

The color adsorption onto different sorbents (nZVI, AC, and GT-nZVI) was studied by batch technique at diverse operating parameters, for instance, pH: 1-12, dose: 0.05-1.0 g, stirring rate: 50-400 rpm, and contact time: 10-120 minutes. A known weight of adsorbent of 0.7 g was equilibrated with 1000 mL of an aqueous color solution of known concentrations (50-350 mg/L Pt/Co) in 1000 mL of Erlenmeyer flasks and then shaked at a known period of time at ambient temperature. After equilibration, the suspension of the adsorbent was detached using a rapid sand filter, and the remained concentrations were measured using spectrophotometer method according to *Standard Methods for the Examination of Water and Wastewater* (23rd edition).[46] The percentage of removal efficiency was calculated using equation (2). The amount of sorbed color was calculated using equation (3):[41]

$$Sorption\ (\%) = \left(\frac{C_0 - C_e}{C_0}\right) \times 100 \qquad (2)$$

where C_0 is the initial concentration (mg/L Pt/Co) and C_e is the equilibrium concentration in solution (Pt/Co):

$$Q_e\ (mg/mg) = \frac{(C_0 - C_e)V}{m} \qquad (3)$$

where Q_e is the equilibrium adsorption capacity (mg/mg), V is the volume of aqueous solution (L), and m is the dry weight of the adsorbent (mg).

Samples collection

Textile wastewater samples were taken before and after receiving coagulation-flocculation and sedimentation treatment process as shown in Figure 1 (Steps 1-11). The samples were collected every single hour over an entire day (grab sampling) to characterize the effluent diversity from local textile mill located at Second Industrial Extend Zone-El-Sadat City, Menoufia-Egypt (30°21′42.9″N, 30°32′55.4″E). Then, the collected samples were reserved in unreacted plastic containers at 4°C overnight to avoid compound degradation and then transported to the laboratory for characterization.

Characterization of nZVI and GT-nZVI

A prepared nanoparticle was characterized using X-ray powder diffraction (XRD) by adding nanopowder sample in XRD machine holder, and then, the X-ray patterns were recorded at a radiation equal to 1.5418 A° (Cu-Kα), with voltage and current values of 40 mA and 40 kV, respectively. While the diffraction angle (2θ) extended from 0° to 80° at a step size of 0.0167°,[47] scanning electron microscope (SEM) with energy-dispersive X-ray (EDX) analysis was performed to obtain the morphology and composition of the nanoparticles. Finally, the UV-Vis scanning spectrum from 190:1000 nm was performed to ensure the absence of impurities and hydroxides during the preparation process.[48,49]

Isotherm studies

Different nonlinear isotherm models were conducted to describe the decolourization process into different sorbent materials including the most common 9 nonlinear equations of Freundlich, Langmuir, Redlich-Peterson, Hill, Sips, Khan, Toth, Koble-Corrigan, and Jovanovic as shown in Supplementary Table 1 (Table S1).[50]

Kinetic studies

To determine the exact time to reach an equilibrium state, Pt/Co color solutions were placed in contact with sorbent

Table 1. The effect of pH, sorbent dose, contact time, stirring rate, and initial color concentration for textile wastewater treatment at temperature 25°C ± 3°C.

	ADSORBENT DOSE (G)	CONTACT TIME (MINUTES)			PH			STIRRING RATE (RPM)			CONCENTRATION (MG/L PT/CO)
	NZVI, AC, AND GT-NZVI	NZVI	AC	GT-NZVI	NZVI	AC	GT-NZVI	NZVI	AC	GT-NZVI	NZVI, AC, AND GT-NZVI
Effect of pH	0.7	50	70	40	1:12						350
Effect of adsorbent dose	0.05:1	50	70	40	5	8	7	150	250	150	350
Effect of contact time	0.7	10:120			5	8	7	150	250	150	350
Effect of stirring rate	0.7	50	70	40	5	8	7	50:400			350
Effect of concentration	0.7	50	70	40	5	8	7	150	250	150	50:350

Abbreviations: AC, activated carbon; GT-nZVI, green synthesized nano zerovalent iron; nZVI, nano zerovalent iron.
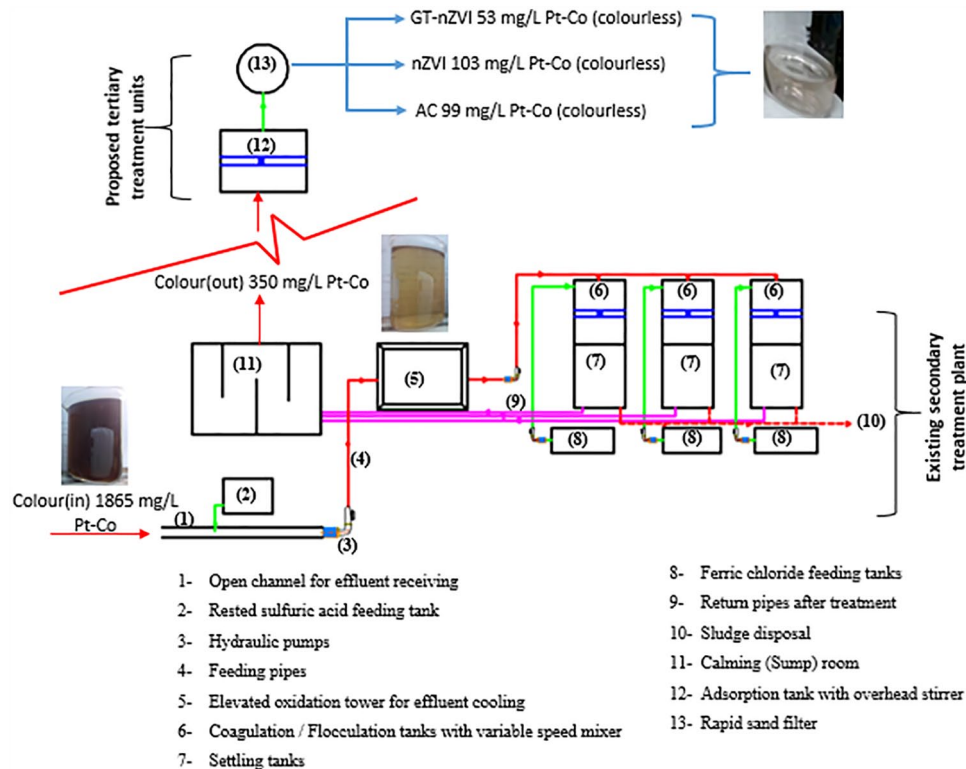
Figure 1. Schematic diagram of existing and proposed treatment units with color inlet and outlet concentrations.

materials at different times at room temperature. The amount of color removed at time t, Q_t (mg/mg), was considered using equation (4)[51]:

$$Q_t = \frac{(C_o - C_t)V}{W} \quad (4)$$

where C_o is the initial concentration (mg/L), C_t is the initial concentration at time t (mg/L), V is the volume of the solution (L), and W is the sorbent dosages.

The kinetic process is investigated using pseudo first-order and second-order, Avrami, Elovich, and Intraparticle as shown in Supplementary Table S2 (Table S2).[52-56]

Statistical analysis

Response surface methodology. The RSM results were carried out using linear regression enter method to predict removal equation, which is important to use all and not restricted on optimum conditions by using equation (5):

Figure 2. (A) SEM result for nZVI with size between 31 and 60 nm, (B) EDAX analysis of the prepared nZVI, (C) SEM analysis for GT-nZVI with size between 60 and 80 nm, and (D) EDAX analysis of the prepared GT-nZVI. EDX indicates energy-dispersive X-ray; GT-nZVI, green synthesized nano zerovalent iron; nZVI, nano zerovalent iron; SEM, scanning electron microscopy.

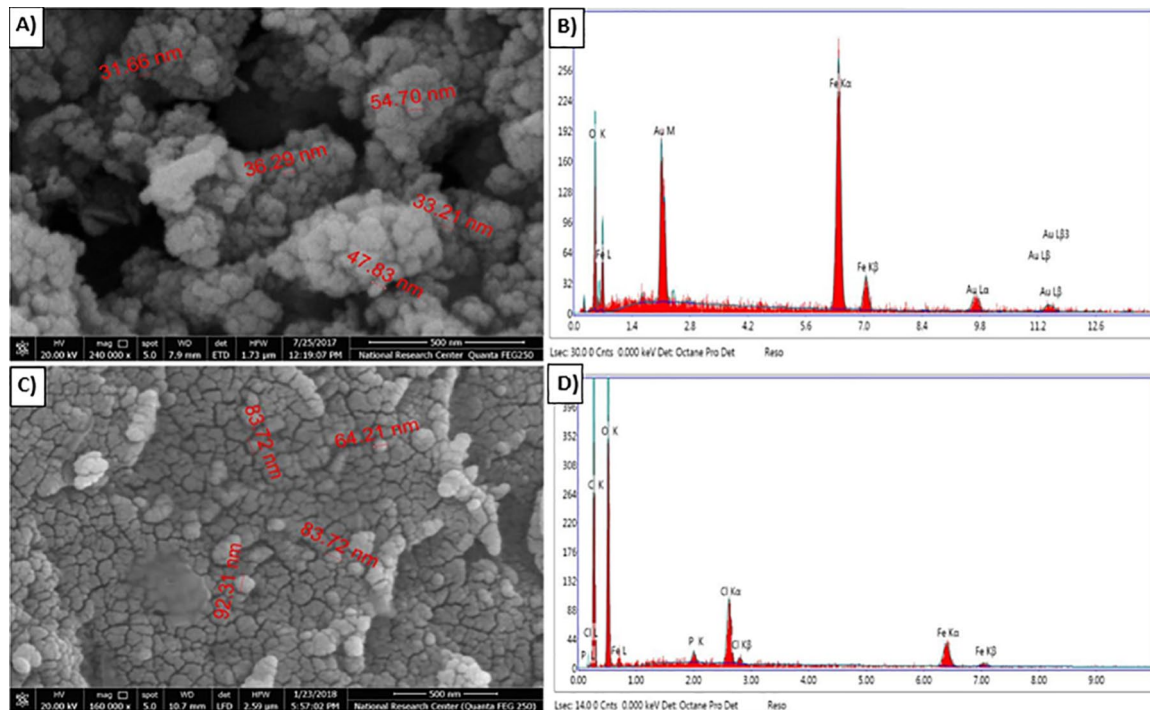$$Y = \beta_0 + \beta_1 x_1 + \beta_2 x_2 + \beta_3 x_3 + \beta_4 x_4 + \beta_5 x_5 + \beta_6 x_6 \qquad (5)$$

where Y is the predicted removal percentages for color removal (%), x_1 is the pH (1-12), x_2 is the dose (0.05-1.0 g), x_3 is time (10-120 minutes), x_4 is the stirring rate (50-400 rpm), x_5 is the initial color concentration (50-350 mg/L Pt/Co), β_0 is the model intercept, and β_1, β_2, β_3, β_4, and β_5 are the linear coefficients of x_1, x_2, x_3, x_4, and x_5, respectively.

Neural network structure. An artificial neural network (ANN) using MLP was established to predict the importance of each operating parameter and build the neural architecture to help to understand the color removal and training artificial results to ensure the tested results. Artificial neural networks of input, hidden, and output layers were used to build artificial architecture. The data from the 5 independent coverable (pH, dose, time, stirring rate, and concentration) are shifted to the input layer. All the obtainable data are generally distributed into standard values for training 70%, validation, and testing 30% procedures and plotted by the system. The network type is multilayer perceptron backpropagation and it is one of the best commonly used neural network architectures.[44,57]

Results and Discussions

Characterization of nZVI and GT-nZVI

Figure 2A displays the SEM characterization image of the prepared powder nZVI before treatment. The nZVI formed regular as well as irregular surface structure with an average size of 40 nm. Many pores were detected, which permits improved mass transfer and diffusion of color into the inner iron nanoparticles.[58] Figure 2B shows EDX analysis of selected nZVI with particle size of 36 nm indicating that the main product in the prepared sample is iron.

Figure 2C shows the SEM characterization image of the prepared GT-nZVI before decolourization process. The formed GT-nZVI with the regular and irregular surface structure showed an average size of 80 nm. Figure 2D shows EDX analysis of selected GT-nZVI with particle size 83.7 nm indicating that the formation of nano Iron is covered by carbon and oxygen layer formed from the green extract. The outer carbon surface acts as AC to adsorb a huge amount of color compounds.

Figure 3A shows the XRD for the powder nZVI in the zero-valent state. The position of the peaks fitted well to the body-centered structure of Fe mineral (JCPDS card No. 87-0722) with diffraction angles 44.713° and 64.9° imputed to (110) and (200) planes, respectively. Also, this figure indicated that there is not any formation of oxides and hydroxides formed during the preparation process. Figure 3B shows the UV-Vis scanning spectrum of nZVI sample in extra pure ethanol at a wavelength between 190 and 1000 nm with a rate of 50 nm/min. This scanning spectrum indicates the formation of the adsorption peaks at 192 and 195 nm indicating the formation of nZVI with an average size between 10 and 100 nm (the main beak was observed at high energy levels of scanning spectrum).[59] Also, the absence of other peaks during the spectrum shows that the formed nZVI in a pure form and the
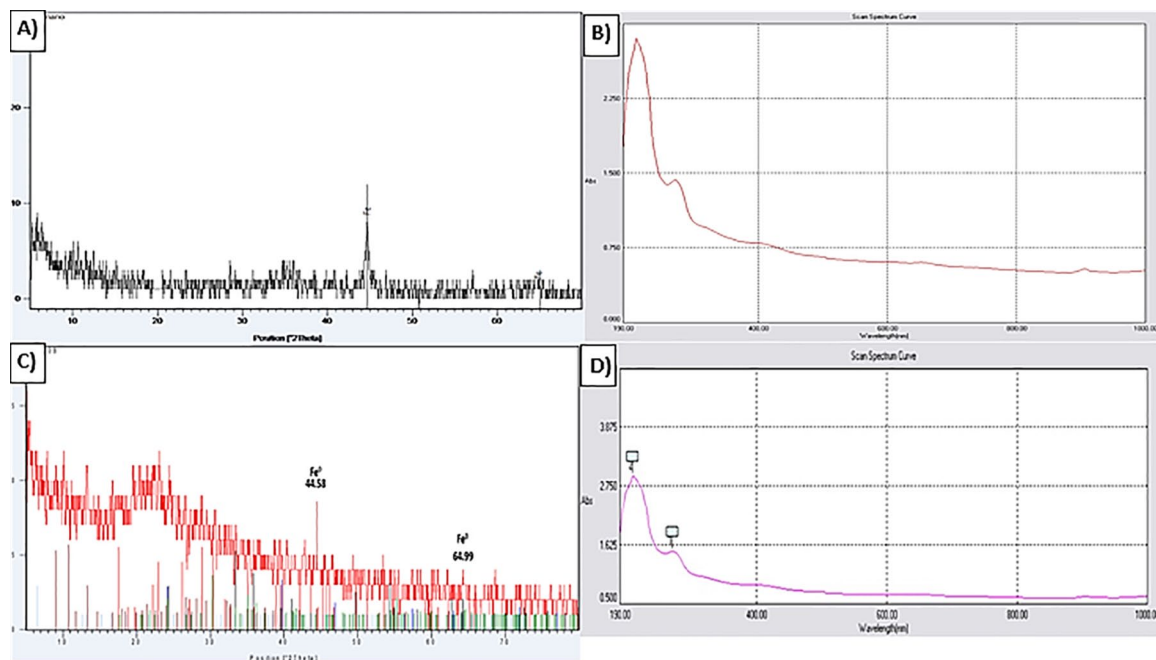
Figure 3. (A) XRD result for chemically prepared nZVI, (B) UV-Vis scanning for nZVI, (C) XRD result for green nZVI (GT-nZVI), and (D) UV-Vis scanning for the GT-nZVI. GT-nZVI indicates green synthesized nano zerovalent iron; nZVI, nano zerovalent iron; XRD, X-ray diffraction.

washing process prevents oxidation and formation of other by-products during the preparation-storage process.

Figure 3C of the XRD result shows 2 main peaks at $2\theta = 44.59°$ and $64.99°$ indicating the formation of pure nano iron powder and showing agreement with the other previous studies. All characterized results agree with previous preparations of a commercial product of nZVI. Figure 3D indicates no creation of oxides and hydroxides during the preparation-storage process.

Effect of operating parameters

Effect of pH. The effect of pH was considered at diverse pH values at acidic, neutral, and alkaline media ranged from 1 to 12 as displayed in Figure 4A. The obtained results suggested that nZVI, AC, and GT-nZVI are effective for color elimination from textile effluents where the removal efficiency were 61%, 63%, 67%, 70%, 71%, 69%, 67%, 61%, 59%, 56%, 51%, and 44% after using nZVI, 46%, 55%, 58%, 61%, 64%, 67%, 70%, 72%, 70%, 69%, 64%, and 62% after using AC, and 71%, 75%, 78%, 81%, 83%, 84%, 85%, 84%, 83%, 81%, 78%, and 74% after using GT-nZVI using diverse pH values (1, 2, 3, 4, 5, 6, 7, 8, 9, 10, 11, and 12), respectively. The obtained results presented that the effective pH for greatest removal efficiency was occurred at 5, 8, and 7 after using nZVI, AC, and GT-nZVI, respectively. The existing textile color comes from both cationic and anionic coloring salts, which can be adsorbed by chemical adsorption process depending on the surface charge (negative or positive). Also, the other disperse dyes can be adsorbed using physical adsorption process. When the surface charge remains neutral, it can reach the point of zero charge (PZC), as well as it is the most suitable condition for the physical adsorption process. The PZC of the prepared nZVI is usually within pH 6-8 exactly at pH 7.7, above PZC result the surface will be charged with negative ions which making a repulsion force between negative ions and electrostatic attraction between positive ions.[60-62] The PZC values determined for AC indicate their acidic nature, which means the charge of AC surface is neutral in slightly alkaline media.[63] Also, powder accumulation may affect the removal efficiency results because it can affect particle mobility and reactivity causing a decrease in the sorbent materials surface area.[64,65] Similarly, the optimum removal for methylene blue was achieved at pH 7.2 by adsorption on different types of commercial AC.[66]

Effect of adsorbent dose. The effect of adsorbent materials dose was studied using different doses ranged from 0.05 to 1 g/L as shown in Figure 4C. The achieved results show that the removal efficiency increased by dose increase where the removal efficiency was 23%, 34%, 41%, 47%, 54%, 59%, 62%, 66%, 71%, 74%, 77%, and 78% after using nZVI; 40%, 45%, 49%, 53%, 57%, 59%, 63%, 66%, 72%, 75%, 78%, and 81% after using AC; and 46%, 54%, 72%, 75%, 77%, 80%, 82%, 83%, 85%, 87%, 90%, and 93% after using GT-nZVI using different doses (0.05, 0.1, 0.2, 0.3, 0.4, 0.5, 0.6, 0.7, 0.8, 0.9, and 1 g/L), respectively. The minimum effective dose for best removal efficiency was 0.7 g/L. The removal efficiency was improved with dose, thanks to getting higher vacant site for adsorption and free electrons for degradation process.[50,67,68]

Effect of contact time. The influence of contact time was considered at different times from 10 to 120 minutes as
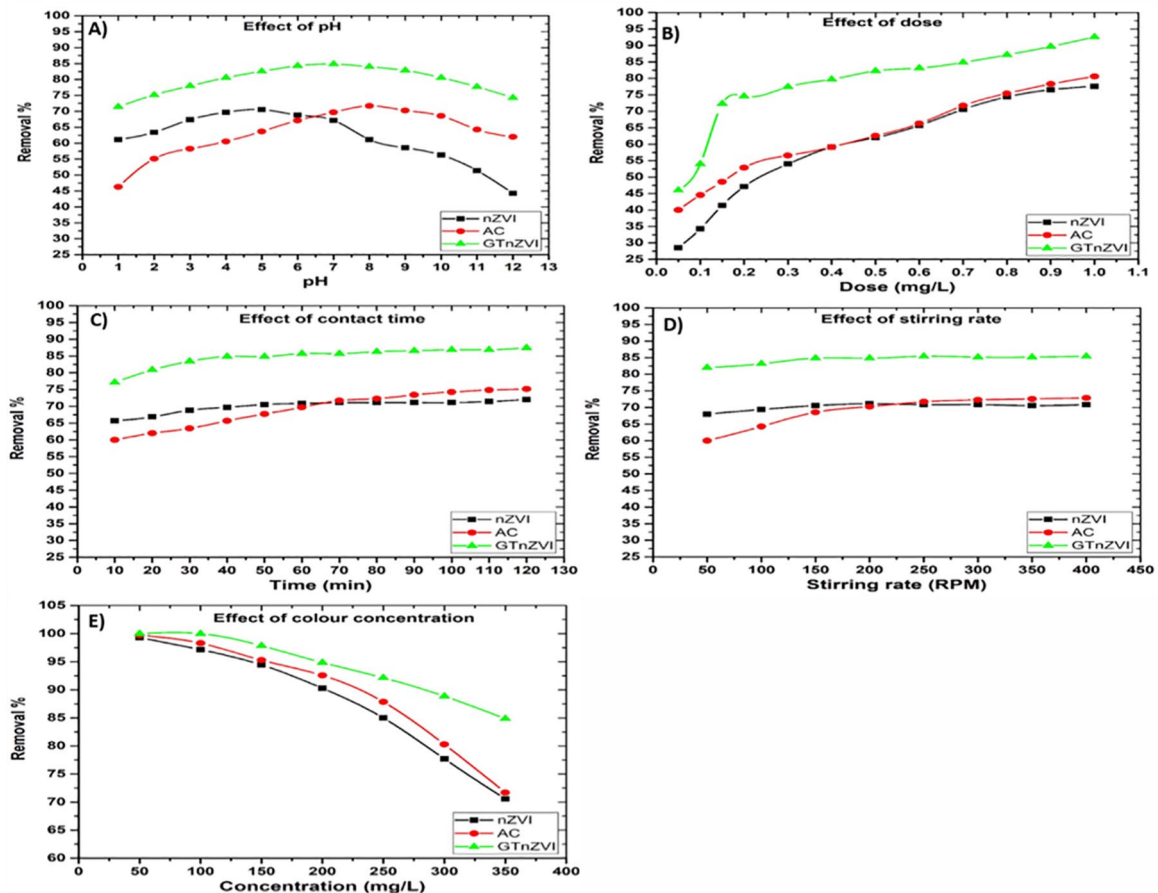
Figure 4. Effect of operating parameter for color removal after using nZVI, AC, and GT-nZVI. (A) Effect of pH on color removal from textile wastewater using nZVI, AC, and GT-nZVI. (B) Effect of adsorbent on color removal from textile wastewater using nZVI, AC, and GT-nZVI. (C) Effect of contact time on color removal from textile wastewater using nZVI, AC, and GT-nZVI. (D) Effect of stirring rate on color removal from textile wastewater using nZVI, AC, and GT-nZVI. (E) Effect of concentration on color removal from textile wastewater using nZVI, AC, and GT-nZVI. AC indicates activated carbon; GT-nZVI, green synthesized nano zerovalent iron; nZVI, nano zerovalent iron.

shown in Figure 4C. The removal efficiency was 66%, 67%, 69%, 70%, 71%, 71%, 71%, 71%, 71%, 71%, 71%, and 72% after using nZVI; 60%, 62%, 63%, 66%, 68%, 70%, 72%, 72%, 73%, 74%, 75%, and 75% after using AC; and 77%, 81%, 83%, 85%, 85%, 86%, 86%, 86%, 87%, 87%, 87%, and 87% after using GT-nZVI at different time (10, 20, 30, 40, 50, 60, 70, 80, 90, 100, 110, and 120 minutes), respectively. The minimum effective time was 50, 70, and 40 minutes after using nZVI, AC, and GT-nZVI, respectively. The methylene blue elimination through AC has been decreased with the enlargement of contact time after 90 minutes, which might also be as a result of the desorption process.[66] Alqadami et al[68] revealed that a 24.3 mg/g adsorption capacity for malachite green dye was achieved using trisodium citrate nanocomposite (Fe_3O_4-TSC) within 40 minutes of contact time at an adsorbent dose of 50 mg/25 mL and a solution pH 7. The initial fast adsorption rate was attributed to the accessibility of large number of binding sites at the exterior surface of the Fe_3O_4-TSC adsorbent. The slow adsorption rates at the end ascribed to the saturation of the binding sites and reaching equilibrium.

Effect of stirring rate. The effect of stirring rate was considered at different stirring rates ranged from 50 to 400 rpm as shown in Figure 4D. The removal efficiency is 68%, 69%, 71%, 71%, 71%, 71%, 71%, and 71% after using nZVI, 60, 64, 69, 70, 72, 72, 73%, and 73% after using AC, 82, 83, 85, 85, 85, 85, 85%, and 85% after using GT-nZVI at diverse stirring rate (50, 100, 150, 200, 250, 300, 350, and 400 rpm), respectively. The minimum effective stirring rate was 150, 250, and 150 rpm after using nZVI, AC, and GT-nZVI, respectively. Similarly, the optimum removal efficiency for methylene blue was achieved at 200 rpm for commercial AC.[69]

Effect of initial color concentration. The effect of initial concentration was considered at different dilutions ranged from 50 to 350 mg/L Pt/Co as shown in Figure 4E. The removal efficiency is 99%, 97%, 94%, 90%, 85%, 78%, and 71% after using nZVI, 100%, 98%, 95%, 93%, 88%, 80%, and 72% after using AC, and 100%, 100%, 98%, 95%, 92%, 89%, and 85% after using GT-nZVI at diverse concentrations (50, 100, 150, 200, 250, 300, and 350 mg/L Pt/Co), respectively. It was detected that the adsorbed rate of dye is better at great concentration initially and then

Table 2. Textile wastewater treatment before and after sorbent additions followed by rapid sand filter for collected samples (*n* = 20).

PARAMETER	UNIT	PARTIALLY TREATED TEXTILE WASTEWATER[a]			TERTIARY TREATMENT STEP			DISCHARGE TO SEWER SYSTEM[b]	DRAINAGE ON NONFRESH WATER BODIES[c]
		MINIMUM	AVERAGE	MAXIMUM	NZVI	AC	GT-NZVI		
pH	—	6	6.25	6.5	6.42	7.18	6.82	6-9.5	6-9
Turbidity	NTU	27	31	34	2.26	3.65	1.92	N/A	<50
COD	mg/L	900	1065	1231	465	569	365	<1100	100
TSS	mg/L	541	621	700	23	29	17	<800	60
TDS	mg/L	532	614	696	632	619	623	N/A	2000
TN	mg/L	22	27	31.2	13	21	16	100	N/A

Abbreviations: AC, activated carbon; COD, chemical oxygen demand; GT-nZVI, green synthesized nano zerovalent iron; nZVI, nano zerovalent iron; TDS, total dissolved salts; TN, total nitrogen; TSS, total suspended solids.
[a]Partially treated textile wastewater: wastewater subjected to coagulation, flocculation, and sedimentation.
[b]Law 93/62 discharge to sewer system (as Decree 44/2000).
[c]Drainage on nonfresh water bodies Law 48/1982.

gradually attains equilibrium. In most cases, it is seen that the initial dye concentration and color removal are contrariwise associated with each other as active sites are saturated if there is high initial concentration. Corda and Kini[69] have done methylene blue removal of 99% and 82.2% with concentration of 50 and 250, respectively, by using sawdust carbon.

Effect of sorbent materials on other wastewater contaminants removal. The effect of nZVI, AC, and GT-nZVI on other textile wastewater was observed for pH, COD, BOD, total dissolved salts (TDS), total suspended solids (TSS), and total nitrogen (TN). Table 2 shows the chemical characterization of the raw and partially treated samples. All analyzed samples were in conflict with the Egyptian Standards for discharging on to sewer systems or non-fresh water bodies. In this study, the average polluted samples were selected to characterize the utmost critical scenario.

Adsorption studies

Table 3 and Figure 5 describe nonlinear relations between different adsorption isotherm models. However, nZVI, AC, and GT-nZVI were represented by A, B, and C symbols. The adsorption isotherms were studied by applying nonlinear equations of Redlich-Peterson, Hill, Sips, Khan, Toth, Koble-Corrigan, Jovanovic, Freundlich, and Langmuir models. The achieved results pointed that the color adsorption onto nZVI meets Hill adsorption isotherm model with the lowest summation of errors 0.162. Hill model describes the binding of diverse categories into homogeneous substrates and supposes that one of the binding places founding into macromolecule can also have an effect on the binding sites in the identical molecule. Consequently, the adsorption process is a supportive phenomenon between adsorbent and adsorbate.[70,71] From the Hill adsorption isotherm, the maximum uptake is 720 mg color/g nZVI as shown in Table 3.

The color adsorption onto AC follows Hill, Sips, and Koble-Corrigan isotherm models with the identical lowermost summation of errors 0.3749. Hill model defines the binding of different types into homogeneous substrates and Sips model describes heterogeneous adsorption isotherm process, which combines Langmuir and Freundlich isotherm models. This model tends to approximate Freundlich model at low concentration and to solve the Freundlich limitation at high concentration through applying Langmuir adsorption model in the prediction of monolayer adsorption showing the maximum uptake is 1299 mg (color)/g (AC) and Koble-Corrigan model describes homogeneous and heterogeneous adsorption mechanisms.

Finally, the adsorption of color onto GT-nZVI obeys both Koble-Corrigan and Freundlich isotherm models with the same lowest summation of errors 1.9414. Koble-Corrigan model combines Langmuir and Freundlich adsorption isotherm models along with the adsorption isotherm for pure color removal. So, the reaction mechanism can be described by Freundlich model.[72] Freundlich model describes heterogeneous adsorption surface and reversible adsorption process, and the multilayer adsorption process can occur in the surface of sorbent materials (GT-nZVI). Also, the adsorption process is influenced by binding energy between adsorbed molecules and sorbent, as well as the adsorption energy declined regularly until vanishes with complete adsorption process.[73] Table 4 describes the relationship between experimental and calculated Q_e after solving nonlinear isotherm equation with constants in Table 3. The values in boldface represent the most suitable isotherm model that can describe the color adsorption onto nZVI, AC, and GT-nZVI.

Kinetic studies

Figure 6 and Table 5 describe the different kinetic model relations. The kinetic analysis was carried by practicing nonlinear

Table 3. Nonlinear adsorption isotherm models results.

Constants	REDLICH-PETERSON (1)	A	B	C	HILL (2)	A	B	C	SIPS (3)	A	B	C	KHAN (4)	A	B	C	TOTH (5)	A	B	C
	Kr	18.0	37.0	34.77	QH	0.72	0.75	1216	Qs	1.299	0.75	3.5	Qk	0.103	0.15	0.166	K_t	0.58	0.571	0.66
	Br	43.2	89.9	67.14	nH	0.60	0.50	0.233	Ks	1.395	8.67	0.0	Bk	365.4	365	365	a_t	0.02	0.014	0.01
	G	2.05	0.22	53.46	KD	0.26	0.33	1583	Bs	0.503	0.50	0.2	Ak	0.656	0.74	0.678	t	0.71	0.698	0.77
Errors		A	B	C		A	B	C		A	B	C		A	B	C		A	B	C
Chi		0.02	0.06	0.999		0.0028	0.0028	0.000		0.0027	0.0992	0.177		0.0014	0.0189	0.8290		0.020	0.0807	0.9901
ERRSQ		0.00	0.00	0.028		0.0005	0.0005	0.000		0.0005	0.0135	0.013		0.0002	0.0012	0.0260		0.001	0.0029	0.0275
HYBRD		0.01	0.02	0.221		0.0028	0.0028	0.000		0.0028	0.0663	0.081		0.0014	0.0127	0.2149		0.012	0.0331	0.2214
MPSD		0.16	0.37	2.021		0.0210	0.0210	0.004		0.0211	0.3711	0.545		0.0142	0.1583	1.9875		0.170	0.4290	2.0209
ARE		0.56	0.86	2.340		0.2972	0.2972	0.135		0.2973	1.1585	1.426		0.2113	0.5761	2.1864		0.564	0.9399	2.3397
EABS		0.06	0.09	0.307		0.0505	0.0505	0.020		0.0505	0.2571	0.256		0.0288	0.0699	0.2650		0.067	0.1034	0.3071
Sum		0.82	1.43	5.916		0.3749	0.3749	0.162		0.3749	1.9658	2.500		0.2573	0.8373	5.5088		0.835	1.5889	5.9068

| Constants	KOBLE-CORRIGAN (6)	A	B	C	JOVANOVIC (7)	A	B	C	FREUNDLICH (8)	A	B	C	LANGMUIR (9)	A	B	C
	A	2.829	2.264	0.650	Q_m	0.338	0.341		K_f	0.922	0.827	0.415	Q_0	0.417	0.398	0.518
	B	3.990	2.989	0.000	K_j	40.35	55.387		n	2.417	2.900	63.254	B	42.7	69.436	67.145
	D	0.616	0.507	0.189												
Errors		A	B	C		A	B	C		A	B	C		A	B	C
Chi error		0.000	0.0028	0.0912		0.0442	0.1627			0.0039	0.002	0.8457		0.0201	0.0807	0.9973
ERRSQ		0.000	0.0005	0.0129		0.0024	0.0049			0.0009	0.000	0.0293		0.0011	0.0029	0.0275
HYBRD		0.000	0.0028	0.0632		0.0237	0.0518			0.0039	0.003	0.2292		0.0125	0.0331	0.2214
MPSD		0.005	0.0210	0.3538		0.2999	0.6349			0.0223	0.028	2.0584		0.1701	0.4290	2.0209
ARE		0.143	0.2972	1.1667		0.8566	1.2438			0.3567	0.343	2.4598		0.5646	0.9399	2.3397
EABS		0.021	0.0505	0.2536		0.1108	0.1499			0.0707	0.053	0.3375		0.0673	0.1034	0.3071
Error sum		0.171	0.3749	1.9414		1.3375	2.2481			0.4585	0.431	5.9599		0.8357	1.5889	5.9140
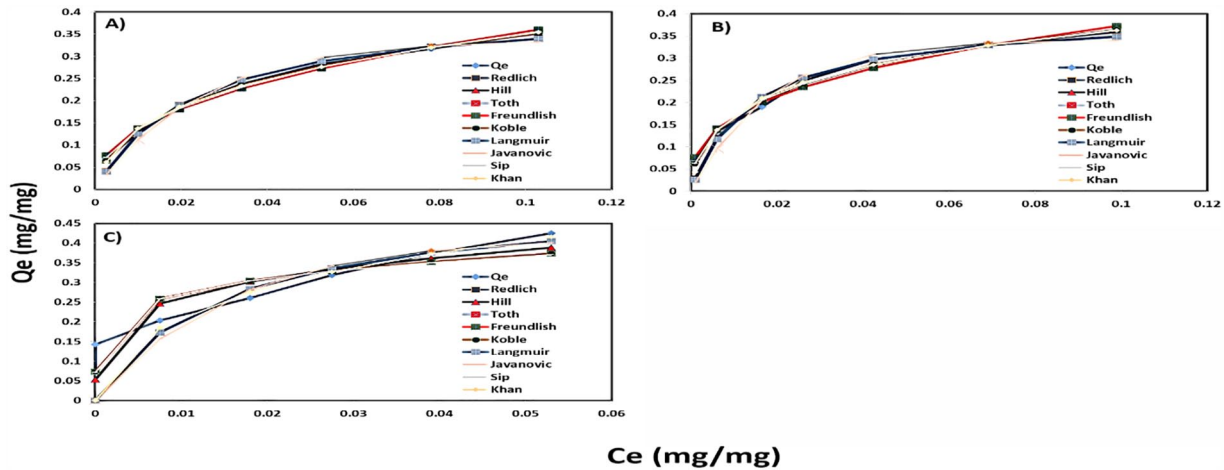
Figure 5. Isotherm studies for color removal after using nZVI, AC, and GT-nZVI. (A) Isotherm studies for color removal from textile wastewater by using nZVI. (B) Isotherm studies for color removal from textile wastewater by using AC. (C) Isotherm studies for color removal from textile wastewater by using GT-nZVI. AC indicates activated carbon; GT-nZVI, green synthesized nano zerovalent iron; nZVI, nano zerovalent iron.

Table 4. Experimental and calculated Q_e for color removal using nZVI, AC and GT-nZVI.

AFTER USING NZVI									
	CALC. Q_E (1)	CALC. Q_E (2)	CALC. Q_E (3)	CALC. Q_E (4)	CALC. Q_E (5)	CALC. Q_E (6)	CALC. Q_E (7)	CALC. Q_E (8)	CALC. Q_E (9)
0.068	0.041	0.065	0.071	0.062	0.040	0.064	0.032	0.077	0.040
0.129	0.126	0.135	0.136	0.138	0.125	0.134	0.112	0.137	0.125
0.186	0.190	0.185	0.182	0.186	0.190	0.185	0.184	0.181	0.190
0.237	0.248	0.235	0.231	0.234	0.247	0.235	0.252	0.228	0.247
0.282	0.289	0.279	0.275	0.276	0.288	0.279	0.297	0.273	0.288
0.317	0.321	0.321	0.321	0.320	0.321	0.321	0.323	0.321	0.321
0.353	0.339	0.352	0.355	0.354	0.340	0.352	0.332	0.360	0.340
AFTER USING AC									
EXP. Q_E	CALC. Q_E (1)	CALC. Q_E (2)	CALC. Q_E (3)	CALC. Q_E (4)	CALC. Q_E (5)	CALC. Q_E (6)	CALC. Q_E (7)	CALC. Q_E (8)	CALC. Q_E (9)
0.070	0.028	0.062	0.062	0.043	0.026	0.062	0.018	0.076	0.026
0.134	0.120	0.138	0.138	0.138	0.117	0.138	0.096	0.142	0.117
0.191	0.212	0.206	0.206	0.210	0.213	0.206	0.204	0.201	0.213
0.249	0.255	0.242	0.242	0.245	0.256	0.242	0.260	0.235	0.256
0.296	0.296	0.285	0.285	0.285	0.298	0.285	0.309	0.278	0.298
0.330	0.330	0.330	0.330	0.328	0.330	0.330	0.334	0.329	0.330
0.359	0.349	0.364	0.364	0.363	0.348	0.364	0.340	0.372	0.348
AFTER USING GT-NZVI									
EXP. Q_E	CALC. Q_E (1)	CALC. Q_E (2)	CALC. Q_E (3)	CALC. Q_E (4)	CALC. Q_E (5)	CALC. Q_E (6)	CALC. Q_E (7)	CALC. Q_E (8)	CALC. Q_E (9)
0.071	0.000	0.053	0.071	0.001	0.000	0.074	0.000	0.074	0.000
0.143	0.000	0.053	0.071	0.001	0.000	0.074	0.000	0.074	0.000

(Continued)

Table 4. (Continued)

AFTER USING GT-NZVI									
EXP. Q_E	CALC. Q_E (1)	CALC. Q_E (2)	CALC. Q_E (3)	CALC. Q_E (4)	CALC. Q_E (5)	CALC. Q_E (6)	CALC. Q_E (7)	CALC. Q_E (8)	CALC. Q_E (9)
0.204	0.173	0.246	0.258	0.186	0.173	0.258	0.157	0.258	0.173
0.260	0.283	0.302	0.304	0.276	0.283	0.304	0.282	0.304	0.283
0.318	0.336	0.333	0.328	0.327	0.336	0.330	0.342	0.330	0.336
0.373	0.375	0.361	0.350	0.372	0.375	0.352	0.380	0.352	0.375
0.424	0.404	0.388	0.370	0.416	0.404	0.373	0.400	0.373	0.404

Abbreviations: AC, activated carbon; GT-nZVI, green synthesized nano zerovalent iron; nZVI, nano zerovalent iron.
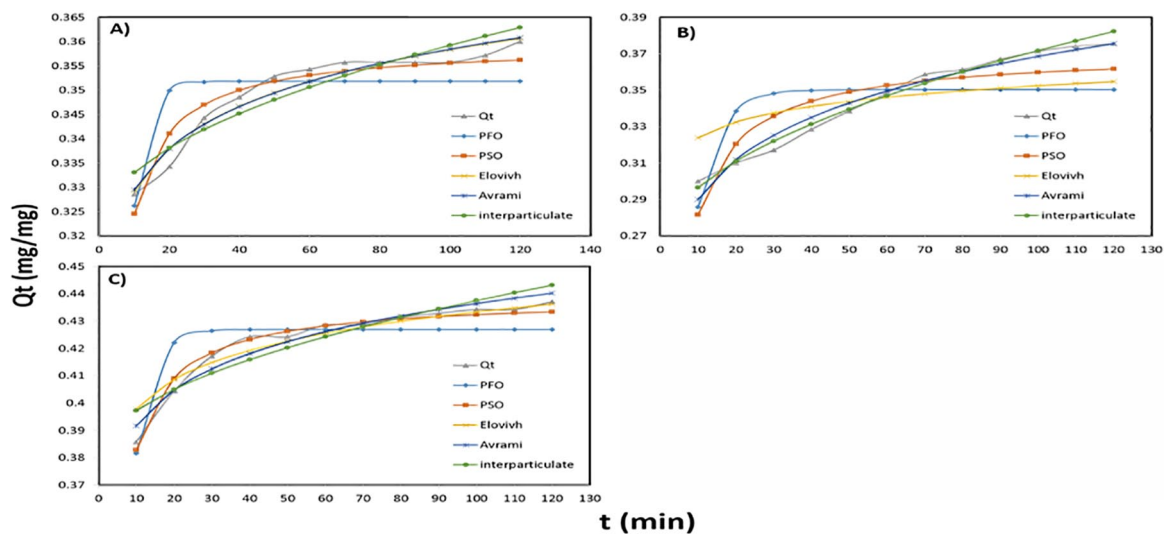

Figure 6. Kinetic studies for color removal after using nZVI, AC, and GT-nZVI. (A) Kinetic studies for color removal from textile wastewater by using nZVI. (B) Kinetic studies for color removal from textile wastewater by using AC. (C) Kinetic studies for color removal from textile wastewater by using GT-nZVI. AC indicates activated carbon; GT-nZVI, green synthesized nano zerovalent iron; nZVI, nano zerovalent iron.

equations of pseudo-first-order (PFO), pseudo-second-order (PSO), Elovich, Avrami, and intraparticle kinetic models. The obtained results indicated that nZVI accepts the Elovich kinetic model with the lowest summation of errors equals to 0.086 as shown in Table 5. Recently, the Elovich model has been used to describe contaminants that are transferring from the aqueous solution to the solid phase as explained in Table S2.

In the case of AC, the kinetic model that can describe kinetic mechanisms is the intraparticle model with the lowest summation of errors equal to 0.124, which means that the adsorbate can transport from the aqueous solution phase to the solid phase of AC as sorbent through an intraparticle diffusion process. Also, this model takes into consideration the mass transfer resistance inside the adsorbent particles and neglects film diffusion.

In the case of GT-nZVI, the kinetic model which can describe kinetic mechanisms is pseudo-second-order model with the lowest summation of errors equal to 0.074, which means that the reaction is more likely to be chemisorption.

Table 6 describes the relation between experimental and calculated Q_t after solving nonlinear kinetic equations with the existing constants in Table 5. The values in boldface represent the most suitable kinetic model that can describe the adsorption kinetic mechanisms if color adsorption onto nZVI, AC, and GT-nZVI at the optimum times.

Statistical analysis

Response surface methodology. The effect of pH, adsorbent dose, contact time, stirring rate, and initial concentration in the textile effluent color removal efficiency is listed in Table 7. In the case of the effect of nZVI and GT-nZVI, positive linear effect of the independent effects "pH," "dose," and "concentration" were observed to be significant at $P < .05$. However, insignificant effect ($P > .05$) was determined for "contact time" and "stirring rate" indicating high reactivity and good dispersed effect of nZVI toward color removal.

In the case of the effect of AC, positive linear effect of the independent effects such as "pH," "dose," "contact time," "stirring rate," and "concentration" was observed to be significant at $P < .05$ indicating that the color removal depends on all effect together.

Table 5. The results of different kinetic models.

Constants

Model	Symbol	A	B	C
PFO (MODEL 1)	Q_e	0.35	0.35	0.43
	K_1	0.26	0.17	0.22
PSO (MODEL 2)	Q_e	0.36	0.37	0.44
	K_2	2.59	0.84	1.56
ELOVICH (MODEL 3)	α	2.43E08		
	β	78.92	80.27	64.8
AVRAMI (MODEL 4)	Q_e	5.97	5.97	5.98
	K_{av}	5.98	0.06	0.05
	N_{av}	5.98	0.06	0.05
INTRAPARTICLE (MODEL 5)		0.06	0.011	0.01
		0.38	0.26	0.38

ERRORS

	PFO (MODEL 1) A	B	C	PSO (MODEL 2) A	B	C	ELOVICH (MODEL 3) A	B	C	AVRAMI (MODEL 4) A	B	C	INTRAPARTICLE (MODEL 5) A	B	C
Chi	0.001	0.014	0.002	0.000	0.005	0.000	0.000	0.010	0.001	0.000	0.001	0.000	0.000	0.000	0.001
ERRSQ	0.000	0.004	0.001	0.000	0.002	0.000	0.000	0.003	0.000	0.000	0.000	0.000	0.000	0.000	0.000
HYBRD	0.001	0.014	0.002	0.000	0.005	0.000	0.000	0.010	0.001	0.000	0.001	0.000	0.000	0.000	0.001
MPSD	0.004	0.041	0.004	0.001	0.016	0.000	0.000	0.030	0.001	0.000	0.003	0.001	0.001	0.001	0.002
ARE	0.176	0.629	0.178	0.074	0.391	0.052	0.063	0.544	0.083	0.066	0.133	0.080	0.108	0.091	0.127
EABS	0.061	0.215	0.075	0.026	0.132	0.022	0.022	0.185	0.034	0.023	0.044	0.033	0.038	0.031	0.053
Sum	0.244	0.917	0.262	0.102	0.551	0.074	0.086	0.782	0.120	0.090	0.181	0.114	0.148	0.124	0.184

Abbreviations: PFO, pseudo first order; PSO, pseudo second order.

Table 6. Experimental and calculated Q_t for color removal using nZVI, AC, and GT-nZVI.

TIME	AFTER USING NZVI						AFTER USING AC						AFTER USING GT-NZVI					
	EXP Q_t	M1	M2	M3	M4	M5	EXP Q_t	M1	M2	M3	M4	M5	EXP Q_t	M1	M2	M3	M4	M5
10	0.329	0.326	0.325	0.329	0.329	0.333	0.300	0.286	0.282	0.324	0.290	0.296	0.386	0.382	0.383	0.398	0.392	0.397
20	0.334	0.350	0.341	0.338	0.338	0.338	0.310	0.338	0.320	0.332	0.312	0.311	0.404	0.422	0.409	0.409	0.405	0.405
30	0.344	0.352	0.347	0.343	0.343	0.342	0.317	0.348	0.336	0.338	0.325	0.322	0.417	0.426	0.418	0.415	0.412	0.411
40	0.349	0.352	0.350	0.347	0.347	0.345	0.329	0.350	0.344	0.341	0.335	0.331	0.424	0.427	0.423	0.419	0.418	0.416
50	0.353	0.352	0.352	0.350	0.349	0.348	0.339	0.350	0.349	0.344	0.343	0.339	0.424	0.427	0.426	0.423	0.422	0.420
60	0.354	0.352	0.353	0.352	0.352	0.351	0.349	0.350	0.353	0.346	0.350	0.347	0.429	0.427	0.428	0.426	0.426	0.424
70	0.356	0.352	0.354	0.354	0.354	0.353	0.359	0.350	0.355	0.348	0.355	0.354	0.429	0.427	0.430	0.428	0.429	0.428
80	0.356	0.352	0.355	0.356	0.356	0.355	0.361	0.350	0.357	0.350	0.360	0.360	0.431	0.427	0.431	0.430	0.432	0.431
90	0.356	0.352	0.355	0.357	0.357	0.357	0.367	0.350	0.359	0.351	0.365	0.366	0.433	0.427	0.432	0.432	0.434	0.435
100	0.356	0.352	0.356	0.358	0.358	0.359	0.371	0.350	0.360	0.353	0.369	0.372	0.434	0.427	0.432	0.433	0.436	0.438
110	0.357	0.352	0.356	0.360	0.360	0.361	0.374	0.350	0.361	0.354	0.372	0.377	0.434	0.427	0.433	0.435	0.438	0.440
120	0.360	0.352	0.356	0.361	0.361	0.363	0.376	0.350	0.362	0.355	0.376	0.382	0.437	0.427	0.433	0.436	0.440	0.443

Abbreviations: AC, activated carbon; GT-nZVI, green synthesized nano zerovalent iron; nZVI, nano zerovalent iron.

Table 7. t statistics and P values for coefficients of the pure linear regression model.

VARIABLE	TERM	ESTIMATE	STANDARD ERROR	t RATIO	PROB$>$|t|	EFFECT*	MODEL (ENTER/REMOVE)				
							STANDARD ERROR	R^2	ADJUSTED R^2	F	SIG
Color removal using nZVI											
Constant	β_0	80.991	4.971	16.292	0.000	Significant	4.431	0.950	0.903	83.858	<0.001
pH	β_1	−2.040	0.349	−5.850	0.000	Significant					
Ads. dose	β_2	48.721	3.511	13.875	0.000	Significant					
Contact time	β_3	0.057	0.035	1.622	0.112	Insignificant					
Stirring rate	β_4	0.014	0.012	1.206	0.234	Insignificant					
Concentration	β_5	−0.119	0.010	−12.053	0.000	Significant					
Color removal using AC											
Constant	β_0	51.943	6.216	8.356	0.000	Significant	4.041	0.951	0.904	84.800	<0.001
pH	β_1	1.833	0.317	5.776	0.000	Significant					
Ads. dose	β_2	38.366	3.188	12.036	0.000	Significant					
Contact time	β_3	0.140	0.034	4.169	0.000	Significant					
Stirring rate	β_4	0.034	0.012	2.741	0.009	Significant					
Concentration	β_5	−0.121	0.009	−13.505	0.000	Significant					
Color removal using GT-ZVI											
Constant	β_0	64.874	5.316	12.204	0.000	Significant	4.012	0.918	0.842	42.69	<0.001
pH	β_1	1.847	0.459	4.028	0.000	Significant					
Ads. dose	β_2	35.942	3.243	11.082	0.000	Significant					
Contact time	β_3	0.051	0.029	1.733	0.091	Insignificant					
Stirring rate	β_4	0.005	0.011	0.438	0.664	Insignificant					
Concentration	β_5	−0.061	0.009	−6.612	0.000	Significant					

Abbreviations: AC, activated carbon; GT-nZVI, green synthesized nano zerovalent iron; nZVI, nano zerovalent iron.
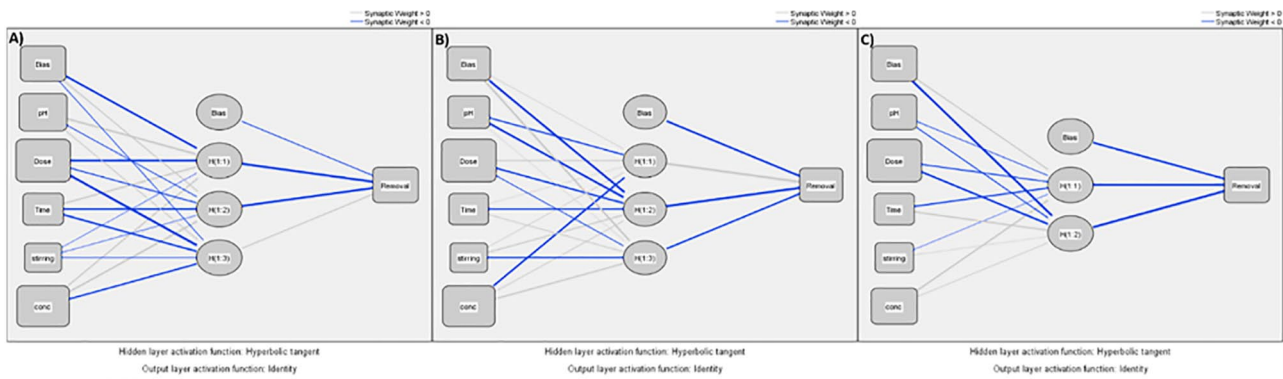
Figure 7. Neural network architecture for color removal after using nZVI, AC, and GT-nZVI. (A) ANN model for color removal using nZVI. (B) ANN model for color removal using AC. (C) ANN model for color removal using GT-nZVI. AC indicates activated carbon; ANN, artificial neural network; GT-nZVI, green synthesized nano zerovalent iron; nZVI, nano zerovalent iron.

The coefficient of determination between measured data and simulated results (R^2), adjusted R^2, F factor, standard error, and P value of each contaminant model were placed in Table 7. The high R^2 value (more than 90% after using nZVI, AC, and GT-nZVI) suggested the reliability of the model. Equation (5) showed all regression models (significant and insignificant):

$$\left(Y\% \text{ after using nZVI}\right) = 80.991 - 2.040\, x_1 + 48.721\, x_2 \\ + 0.057\, x_3 + 0.014\, x_4 - 0.119\, x_5$$

$$\left(Y\% \text{ after using AC}\right) = 51.943 + 1.833\, x_1 + 38.366\, x_2 \\ + 0.140\, x_3 + 0.034\, x_4 - 0.121\, x_5$$

$$\left(Y\% \text{ after using GT-nZVI}\right) = 64.874 + 1.847\, x_1 + 32.942\, x_2 \\ + 0.051\, x_3 + 0.005\, x_4 - 0.061\, x_5,$$

where Y is the predicted response of color removal efficiency (%), x_1 is the contact time (10-120 minutes), x_2 is the adsorbent dose (0.05-1.0 g), x_3 is the pH (1-12), x_4 is the stirring rate (50-400 rpm), color concentration is 50-350 mg/L Pt/Co, β_0 is the model intercept, and β_1, β_2, β_3, β_4, and β_5 are the linear coefficients of x_1, x_2, x_3, x_4, and x_5, respectively.

Artificial neural network. Backpropagation statistical algorithms model was used to build the neural networks architectures. The neural network model adapted operating coverable (pH, dose, time, stirring rate, and concentration) by connecting weight and bias through a continuous progression to build the artificial neural network architectures for color removal (target) as shown in Figure 7.[44,74]

Each color contaminant removal was calculated using training and testing techniques without any excluded as explained in Table 8.

Statistical input, hidden environment, and output layer environment indicated that all sorbent materials run at the same coverable calculation techniques except the number of unit in hidden layers as shown in Table 9.

Table 8. Case processing summary.

PARAMETER	NZVI		AC		GT-NZVI	
	N	%	N	%	N	%
Sample training	28	54.9	39	76.5	36	78.3
Sample testing	23	45.1	12	23.5	10	21.7
Valid	51	100.0	51	100.0	46	100.0
Excluded	0		0		0	
Total	51		51		46	

Abbreviations: AC, activated carbon; GT-nZVI, green synthesized nano zerovalent iron; nZVI, nano zerovalent iron.

Table 10 shows the obtained ANNs of testing and training results indicating that the SSE for all parameter was acceptable showing agreement with RSM results and chemical explanation.

Figure 8A to C shows the relation between the residual results and predictive results indicating that there is no significant difference between them (−7.5%, +5%) after using nZVI, (−15%, +5%) after using AC, and (−15%, +10%) after using GT-nZVI.

Table 11 and Figure 9 show the importance and normalized importance results for each coverable effects on color removal using nZVI, AC, and GT-nZVI. The normalized importance agreed with previous discussions of effect of operating parameter and RSM statistic algorithm.

Conclusions

This study investigates the impact of using nZVI, AC, and GT-nZVI for color adsorption from partially treated fabric wastewater. The maximum environmental conditions for color elimination were pH 5, contact time 50 minutes, and stirring rate 150 rpm for nZVI; pH 8, contact time 70 minutes, and stirring rate 250 rpm for AC; and pH 7, contact time 40 minutes, and stirring rate 150 rpm for GT-nZVI,

Table 9. Network information.

		NZVI	AC	GT-NZVI
Input layer	Covariates	5 (pH, dose, time, stirring rate, and concentration)		
	Number of units	5		
	Rescaling method for covariates	Normalized		
Hidden layer(s)	Number of hidden layers	1		
	Number of units in hidden layer 1	3	3	2
	Activation function	Hyperbolic tangent		
Output layer	Dependent variables	Removal		
	Number of units	1		
	Rescaling method for scale dependents	Standardized		
	Activation function	Identity		
	Error function	Sum of squares		

Abbreviations: AC, activated carbon; GT-nZVI, green synthesized nano zerovalent iron; nZVI, nano zerovalent iron.

Table 10. Model summaries.

	NZVI	AC	GT-NZVI
Training			
Sum of squares error	0.726	0.128	1.636
Relative error	0.054	0.007	0.093
Stopping rule used	One consecutive step(s) with no decrease in error		
Testing			
Sum of squares error	0.175	0.641	0.587
Relative error	0.023	0.111	0.248

Abbreviations: AC, activated carbon; GT-nZVI, green synthesized nano zerovalent iron; nZVI, nano zerovalent iron.
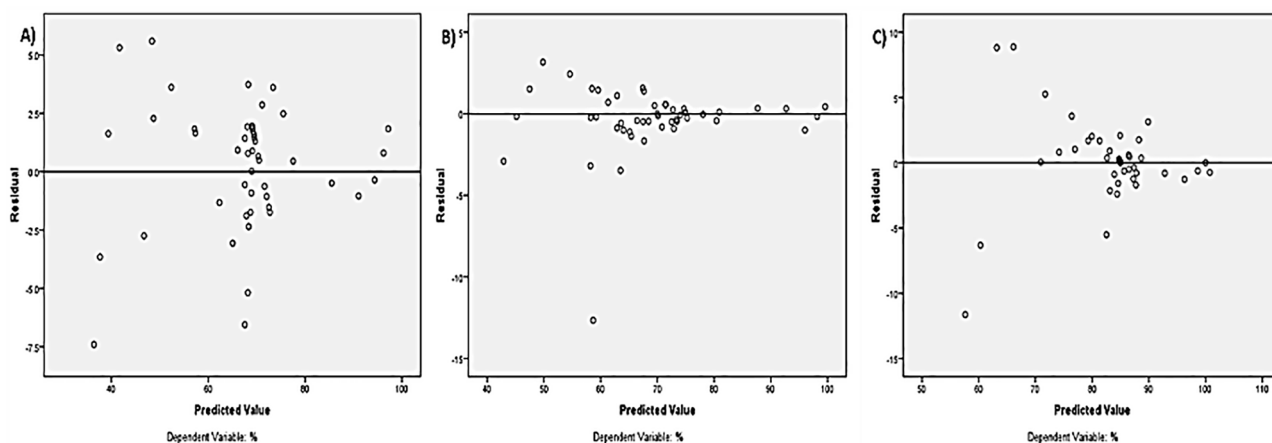

Figure 8. Relation between the residual results and predictive results for color removal after using nZVI, AC, and GT-nZVI. (A) Relation between predicted model and residual model after using nZVI. (B) Relation between predicted model and residual model after using AC. (C) Relation between predicted model and residual model after using GT-nZVI. AC indicates activated carbon; GT-nZVI, green synthesized nano zerovalent iron; nZVI, nano zerovalent iron.

Table 11. Independent variable importance.

	NZVI	AC	GT-NZVI
Importance			
pH	0.227	0.147	0.203
Adsorbent dose	0.363	0.342	0.431
Contact time	0.083	0.119	0.087
Stirring rate	0.010	0.085	0.047
Concentration	0.318	0.306	0.232
Normalized importance			
pH	62.5%	43.1%	47.1%
Adsorbent dose	100.0%	100.0%	100.0%
Contact time	22.8%	34.9%	20.2%
Stirring rate	2.8%	24.8%	10.9%
Concentration	87.6%	89.5%	54.0%

Abbreviations: AC, activated carbon; GT-nZVI, green synthesized nano zerovalent iron; nZVI, nano zerovalent iron.
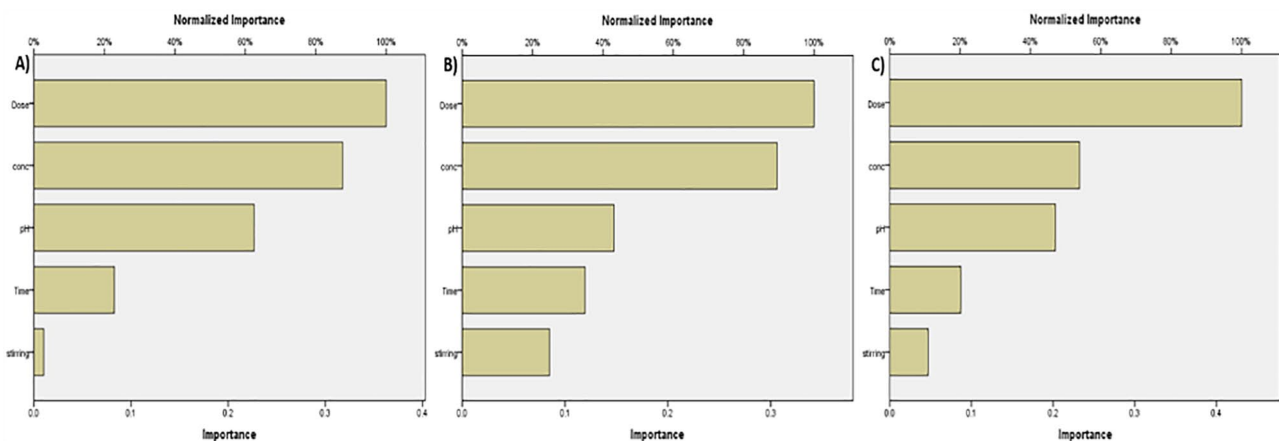

Figure 9. Importance and normalized importance results for color removal after using nZVI, AC, and GT-nZVI. (A) Importance and normalized importance for color removal from textile wastewater using nZVI. (B) Importance and normalized importance for color removal from textile wastewater using AC. (C) Importance and normalized importance for color removal from textile wastewater using GT-nZVI. AC indicates activated carbon; GT-nZVI, green synthesized nano zerovalent iron; nZVI, nano zerovalent iron.

respectively. At constant dose of 0.7 g/L and room temperature concerning the obtained optimum environmental parameters for each sorbent material, the best color removal efficiency for 350 and 50 mg/L Pt/Co color unit was achieved to be 71% and 99%, respectively, after using nZVI; 72% and 100%, respectively, after using AC; and about 85% and 100%, respectively, after using GT-nZVI. The isotherm study pointed that nZVI color adsorption meets Hill adsorption isotherm model. AC color adsorption meets Hill, Sips, and Koble-Corrigan isotherm models. As well as, GT-nZVI color adsorption meets both Koble-Corrigan and Freundlich isotherm models. The kinetic study pointed that nZVI adsorption follows the Elovich kinetic model, AC adsorption the intraparticle model, and GT-nZVI meets pseudo-second-order model. The ANN and RSM models were able to predict and simulate the adsorption process of color. In conclusion, this study suggests the use of GT-nZVI rather than AC or nZVI due to its amazing removal efficiency and simple eco-friendly preparation steps.

Author Contributions

AK contributed to sample collection, system build-up, effect of operating parameters, and ANN modeling by applying nonlinear MLP statistical algorithms writing and reviewing. KZ contributed to error functions analyzing and response surface methodologies regression analysis writing and reviewing. ASM contributed to preparation of nZVI, GT-nZVI preparation, characterization, application of real textile sample, kinetic

and isotherm studies, writing, and reviewing. RSF contributed to kinetic and isotherm studies, writing, and reviewing.

ORCID iDs

Ahmed Karam (iD) https://orcid.org/0000-0002-2075-653X
Ahmed S Mahmoud (iD) https://orcid.org/0000-0003-3092-8056

Supplemental material

Supplemental material for this article is available online.

REFERENCES

1. Ranade VV, Bhandari VM. *Industrial Wastewater Treatment, Recycling and Reuse*. Oxford, UK: Butterworth-Heinemann; 2014.
2. Shiklomanov IA. The world's water resources. In: *Proceedings of the International Symposium to Commemorate 25 Years of the IHP*. Paris, France: United Nations Educational, Scientific and Cultural Organization. Vol. 25. 1991;93-105.
3. United Nations Environment Program (UNEP). *Global Environment Outlook 4 (GEO–4): Environment for Development*. Valletta, Malta: UNEP; 2007.
4. Water UN. Coping with water scarcity: challenge of the twenty-first century. Prepared for World Water Day; 2007. http://www.fao.org/3/a-aq444e.pdf.
5. Nemerow NL. *Industrial Water Pollution: Origins, Characteristics, and Treatment*. Malabar, FL: Robert E. Krieger; 1987.
6. Paul SA, Chavan SK, Khambe SD. Studies on characterization of textile industrial waste water in Solapur city. *Int J Chem Sci*. 2012;10:635-642.
7. Ghaly AE, Ananthashankar R, Alhattab M, Ramakrishnan VV. Production, characterization and treatment of textile effluents: a critical review. *J Chem Eng Process Technol*. 2014;5:1-19.
8. Akar ST, Uysal R. Untreated clay with high adsorption capacity for effective removal of C.I. Acid Red 88 from aqueous solutions: batch and dynamic flow mode studies. *Chem Eng J*. 2010;162:591-598.
9. Puvaneswari N, Muthukrishnan J, Gunasekaran P. Toxicity assessment and microbial degradation of azo dyes. *Indian J Exp Biol*. 2006;44:618-626.
10. Malik A, Grohmann E, Akhtar R. *Environmental Deterioration and Human Health*. Dordrecht, The Netherlands: Springer; 2014.
11. Elawwad A, Karam A, Zaher K. Using an algal photo-bioreactor as a polishing step for secondary treated wastewater. *Pol J Environ Stud*. 2017;26:1493-1500.
12. Sevimli MF, Sarikaya HZ. Ozone treatment of textile effluents and dyes: effect of applied ozone dose, pH and dye concentration. *J Chem Technol Biot*. 2002;77:842-850.
13. Alventosa-deLara E, Barredo-Damas S, Alcaina-Miranda MI, Iborra-Clar MI. Ultrafiltration technology with a ceramic membrane for reactive dye removal: optimization of membrane performance. *J Hazard Mater*. 2012;209:492-500.
14. Tavangar T, Jalali K, Shahmirzadi MAA, Karimi M. Toward real textile wastewater treatment: membrane fouling control and effective fractionation of dyes/inorganic salts using a hybrid electrocoagulation-nanofiltration process. *Sep Purif Technol*. 2019;216:115-125.
15. Ciardelli G, Corsi L, Marcucci M. Membrane separation for wastewater reuse in the textile industry. *Resour Conserv Recy*. 2001;31:189-197.
16. Naushad M, Sharma G, Alothman ZA. Photodegradation of toxic dye using Gum Arabic-crosslinked-poly (acrylamide)/Ni(OH)$_2$/FeOOH nanocomposites hydrogel. *Journal of Cleaner Production*. 2019;241:118263.
17. Kumar A, Naushad M, Rana A, et al. ZnSe-WO3 nano-hetero-assembly stacked on Gum ghatti for photo-degradative removal of Bisphenol A: symbiose of adsorption and photocatalysis. *Int J Biol Macromol*. 2017;104:1172-1184.
18. Elkodous MA, Hassaan A, Ghoneim AI, Abdeen Z. C-dots dispersed macro-mesoporous TiO$_2$ photocatalyst for effective waste water treatment. *Character Appl Nanomater*. 2018;1:1-9.
19. Tatarchuk T, Paliychuk N, Bitra RB, et al. Adsorptive removal of toxic Methylene Blue and Acid Orange 7 dyes from aqueous medium using cobalt-zinc ferrite nanoadsorbents. *Desalin Water Treat*. 2019;150:374-385.
20. Mohanraj J, Durgalakshmi D, Balakumar S, et al. Low cost and quick time absorption of organic dye pollutants under ambient condition using partially exfoliated graphite [published online ahead of print December 13, 2019]. *J Water Proc Eng*. doi:10.1016/j.jwpe.2019.101078.
21. Khan NA, Ibrahim S, Subramaniam P. Elimination of heavy metals from wastewater using agricultural wastes as adsorbents. *Malays J Sci*. 2004;23:43-51.
22. Naushad M, Ahamad T, AlOthman ZA, Al-Muhtaseb AH. Green and eco-friendly nanocomposite for the removal of toxic Hg(II) metal ion from aqueous environment: adsorption kinetics & isotherm modelling. *J Mol Liq*. 2019;279:1-8.
23. Djilali Y, Elandaloussi EH, Aziz A, de Ménorval L-C. Alkaline treatment of

24. Mahmoodi NM, Hayati B, Arami M, Lan C. Adsorption of textile dyes on pine cone from colored wastewater: kinetic, equilibrium and thermodynamic studies. *Desalination*. 2011;268:117-125.
25. Albadarin AB, Collins MN, Naushad M, Shirazian S, Walker G, Mangwandi C. Activated lignin-chitosan extruded blends for efficient adsorption of methylene blue. *Chem Eng J*. 2017;307:264-272.
26. Naushad M, Alqadami AA, Alothman ZA, Alsohaimi IH, Algamdi MS, Aldawsari AM. Adsorption kinetics, isotherm and reusability studies for the removal of cationic dye from aqueous medium using arginine modified activated carbon. *J Mol Liq*. 2019;293:111442.
27. Khellouf M, Chemini R, Salem Z, Khodja M, Zeriri D. Parametric study of COD reduction from textile processing wastewater using adsorption on cypress cone-based activated carbon: an analysis of a Doehlert response surface design. *Arab J Sci Eng*. 2019;44:10079-10086.
28. Ahmad AA, Hameed BH. Reduction of COD and color of dyeing effluent from a cotton textile mill by adsorption onto bamboo-based activated carbon. *J Hazard Mater*. 2009;172:1538-1543.
29. Fan J, Guo Y, Wang J, Fan M. Rapid decolorization of azo dye methyl orange in aqueous solution by nanoscale zerovalent iron particles. *J Hazard Mater*. 2009; 166:904-910.
30. Chen Z-X, Jin X-Y, Chen Z, Megharaj M, Naidu R. Removal of methyl orange from aqueous solution using bentonite-supported nanoscale zero-valent iron. *J Colloid Interface Sci*. 2011;363:601-607.
31. Shu H-Y, Chang M-C, Yu H-H, Chen W-H. Reduction of an azo dye Acid Black 24 solution using synthesized nanoscale zerovalent iron particles. *J Colloid Interf Sci*. 2007;314:89-97.
32. Heberling J, Adewuyi Y, Mahmoud AS, Mostafa M, Peters RW. AOP performance at wastewater treatment plants: recent developments. Paper presented at: Environmental Division 2018—Core Programming Area at the 2018 AIChE Annual Meeting. Pittsburgh, PA, October 28-November 2. 2018:10-21.
33. Wen Z, Zhang Y, Dai C. Removal of phosphate from aqueous solution using nanoscale zerovalent iron (nZVI). *Colloid Surface A*. 2014;457:433-440.
34. Li S, Wang W, Liang F, Zhang W-X. Heavy metal removal using nanoscale zero-valent iron (nZVI): theory and application. *J Hazard Mater*. 2017;322:163-171.
35. Raychoudhury T, Scheytt T. Potential of zerovalent iron nanoparticles for remediation of environmental organic contaminants in water: a review. *Water Sci Technol*. 2013;68:1425-1439.
36. Raman CD, Kanmani S. Textile dye degradation using nano zerovalent iron: a review. *J Environ Manage*. 2016;177:341-355.
37. Hoag GE, Collins JB, Holcomb JL, Hoag JR, Nadagouda MN, Varma RS. Degradation of bromothymol blue by "greener" nano-scale zero-valent iron synthesized using tea polyphenols. *J Mater Chem*. 2009;19:8671-8677.
38. Shahwan T, Sirriah SA, Nairat M, et al. Green synthesis of iron nanoparticles and their application as a Fenton-like catalyst for the degradation of aqueous cationic and anionic dyes. *Chem Eng J*. 2011;172:258-266.
39. Karimifard S, Moghaddam MRA. Application of response surface methodology in physicochemical removal of dyes from wastewater: a critical review. *Sci Total Environ*. 2018;640:772-797.
40. Vargas AMM, Martins AC, Almeida VC. Ternary adsorption of acid dyes onto activated carbon from flamboyant pods (Delonix regia): analysis by derivative spectrophotometry and response surface methodology. *Chem Eng J*. 2012;195:173-179.
41. Mahmoud AS, Farag RS, Elshfai MM. Reduction of organic matter from municipal wastewater at low cost using green synthesis nano iron extracted from black tea: artificial intelligence with regression analysis [published online ahead of print September 10, 2019]. *Egypt J Petroleum*. doi:10.1016/j.ejpe.2019.09.001.
42. Karam A, Mostafa MK, Elawwad A, Zaher K, Mahmoud AS, Peters RW. Small-pilot plant for tertiary treatment of domestic wastewater using algal photo-bioreactor, with artificial intelligence. Paper presented at: AIChE Annual Meeting. Orlando, FL, November 10-15. 2019.
43. Daneshvar N, Khataee AR, Djafarzadeh N. The use of artificial neural networks (ANN) for modeling of decolorization of textile dye solution containing C. I. Basic Yellow 28 by electrocoagulation process. *J Hazard Mater*. 2006;137:1788-1795.
44. Mahmoud AS, Mostafa MK, Nasr M. Regression model, artificial intelligence, and cost estimation for phosphate adsorption using encapsulated nanoscale zero-valent iron. *Sep Sci Technol*. 2019;54:13-26.
45. Farag RS, Elshfai MM, Mahmoud AS, Mostafa MK, Peters RW. Green synthesis of nano iron carbide: preparation, characterization and application for aqueous phosphate removal. Paper presented at: Environmental Division 2018—Core Programming Area at the 2018 AIChE Annual Meeting. Pittsburgh, PA, October 28-November 2. 2018:307-317.
46. Rice EW, Baird RB, Eaton AD, Clesceri LS. *Standard Methods for the Examination of Water and Wastewater*. Washington, DC: APHA, AWWA, WPCR; 2012.

47. Xi Y, Mallavarapu M, Naidu R. Reduction and adsorption of Pb 2+ in aqueous solution by nano-zero-valent iron—a SEM, TEM and XPS study. *Mater Res Bull*. 2010;45:1361-1367.

48. El-Shafei M, Mahmoud A, Mostafa M, Peters R. Effects of entrapped nZVI in alginate polymer on BTEX removal. Paper presented at: AIChE Annual Meeting. San Francisco, CA. 2016:13-18.

49. Mahmoud AS, Ismail A, Mostafa MK, Mahmoud M, Ali W, Shawky AM. Isotherm and kinetic studies for heptachlor removal from aqueous solution using Fe/Cu nanoparticles, artificial intelligence, and regression analysis. *Sep Sci Technol*. 2019;55:684-696.

50. Saryel-Deen RA, Mahmoud AS, Mahmoud M, Mostafa MK, Peters RW. Adsorption and kinetic studies of using entrapped sewage sludge ash in the removal of chemical oxygen demand from domestic wastewater, with artificial intelligence approach. Paper presented at: 2017 Annual AIChE Meeting. Minneapolis, MN, October 29-November 3. 2017.

51. Farag RS, Elshfai MM, Mahmoud AS. Adsorption and kinetic studies using nano zero valent iron (nZVI) in the removal of chemical oxygen demand from aqueous solution with response surface methodology and artificial neural network approach. *J Environ Biotech Res*. 2018;7:12-22.

52. Fola AT, Idowu AA, Adetutu A. Removal of Cu2+ from aqueous solution by adsorption onto quail eggshell: kinetic and isothermal studies. *J Environ Biotech Res*. 2016;5:1-9.

53. Ho YS, Mckay G. Kinetic models for the sorption of dye from aqueous solution by wood. *Process Saf Environ*. 1998;76:183-191.

54. Avrami M. Kinetics of phase change. II transformation-time relations for random distribution of nuclei. *J Chem Phys*. 1940;8:212-224.

55. Zeldowitsch J. Über den mechanismus der katalytischen oxydation von CO an MnO2. *Acta Physicochim URS*. 1934;1:364-449.

56. Ho Y-S, Mckay G. Pseudo-second order model for sorption processes. *Process Biochem*. 1999;34:451-465.

57. Mahmoud AS, Saryel-Deen RA, Mostafa MK, Peters RW. Artificial intelligence for organochlorine pesticides removal from aqueous solutions using entrapped nZVI in alginate biopolymer. Annual AIChE Meeting. Minneapolis, MN, October 29-November 3. 2017.

58. Meda L, Marra G, Galfetti L, Severini FDE, Luca L. Nano-aluminum as energetic material for rocket propellants. *Mater Sci Eng C*. 2007;27:1393-1396.

59. Farahmandjou M, Soflaee F. Synthesis and characterization of α-Fe2O3 nanoparticles by simple co-precipitation method. *Phys Chem Res*. 2015;3:191-196.

60. Kosmulski M. pH-dependent surface charging and points of zero charge II. Update. *J Colloid Interface Sci*. 2004;275:214-224.

61. Bezbaruah AN, Krajangpan S, Chisholm BJ, Khan E, Bermudez JJE. Entrapment of iron nanoparticles in calcium alginate beads for groundwater remediation applications. *J Hazard Mater*. 2009;166:1339-1343.

62. Naushad M, Ahamad T, Al-Maswari BM, Alqadami AA, Alshehri SM. Nickel ferrite bearing nitrogen-doped mesoporous carbon as efficient adsorbent for the removal of highly toxic metal ion from aqueous medium. *Chem Eng J*. 2017;330: 1351-1360.

63. Giraldo L, Moreno-Piraján J. Pb2+ adsorption from aqueous solutions on activated carbons obtained from lignocellulosic residues. *Braz J Chem Eng*. 2008;25: 143-151.

64. Kröger S, Law RJ. Sensing the sea. *Trends Biotechnol*. 2005;23:250-256.

65. Watts M. *Novel Bionanotechnological Approaches for the Remediation of Contaminated Land* [PhD thesis]. The University of Manchester; 2014.

66. Kannan N, Sundaram MM. Kinetics and mechanism of removal of methylene blue by adsorption on various carbons—a comparative study. *Dyes Pigments*. 2001;51:25-40.

67. Gupta VK. Application of low-cost adsorbents for dye removal—a review. *J Environ Manage*. 2009;90:2313-2342.

68. Alqadami AA, Naushad M, Abdalla MA, Khan MR, Alothman ZA. Adsorptive removal of toxic dye using Fe3O4-TSC nanocomposite: equilibrium, kinetic, and thermodynamic studies. *J Chem Eng Data*. 2016;61:3806-3813.

69. Corda NC, Kini MSA. Review on adsorption of cationic dyes using activated carbon. MATEC Web Conf. 2018;144:02022.

70. Ringot D, Lerzy B, Chaplain K, Bonhoure J-P, Auclair E, Larondelle Y. In vitro biosorption of ochratoxin A on the yeast industry by-products: comparison of isotherm models. *Bioresour Technol*. 2007;98:1812-1821.

71. Hill AV. The possible effects of the aggregation of the molecules of haemoglobin on its dissociation curves. *J Physiol*. 1910;40:4-7.

72. Koble RA, Corrigan TE. Adsorption isotherms for pure hydrocarbons. *Ind Eng Chem*. 1952;44:383-387.

73. Redlich O, Peterson DL. A useful adsorption isotherm. *J Phys Chem*. 1959;63: 1024-1024.

74. Mahmoud AS, Farag RS, Elshfai MM, Mohamed LA, Ragheb SM. Nano zerovalent aluminum (nZVAl) preparation, characterization, and application for the removal of soluble organic matter with artificial intelligence, isotherm study, and kinetic analysis. *Air Soil Water Res*. 2019;12:1178-6221.